Article:
Xuan, D., Becker, R., Vargas Valverde, M. et al. (2026) Spatial patterns of glacier-wetland hydrological connectivity in the rapidly deglaciating Peruvian Andes. Earth's Future, 14 (6). e2026EF008149. ISSN: 2328-4277

https://doi.org/10.1029/2026ef008149

ADVANCING EARTH AND SPACE SCIENCES

Earth's Future

RESEARCH ARTICLE
10.1029/2026EF008149

Spatial Patterns of Glacier-Wetland Hydrological Connectivity in the Rapidly Deglaciating Peruvian Andes

D. Xuan[1], R. Becker[1], M. Vargas Valverde[2], B. J. Davies[3], J. C. Ely[4], O. King[3], N. Montoya[2], C. Onof[1], A. C. Ross[1], and W. Buytaert[1]

[1]Department of Civil and Environmental Engineering, Imperial College London, London, UK, [2]Departamento Académico de Agricultura, Universidad Nacional de San Antonio Abad del Cusco, Cusco, Peru, [3]School of Geography, Politics and Sociology, Newcastle University, Newcastle-upon-Tyne, UK, [4]School of Geography and Planning, University of Sheffield, Sheffield, UK

Dingyu Xuan and Rike Becker contributed equally to this work and share first authorship.

Key Points:

- Precipitation-derived water is the primary driver of wetland wetting and drying
- Glaciers attenuate the seasonal wetting and drying of nearby wetlands, but this effect reduces with downstream distance
- Glacier retreat may increase the sensitivity of nearby wetlands to precipitation changes

Supporting Information:

Supporting Information may be found in the online version of this article.

Correspondence to:

R. Becker,
r.becker@imperial.ac.uk

Citation:

Xuan, D., Becker, R., Vargas Valverde, M., Davies, B. J., Ely, J. C., King, O., et al. (2026). Spatial patterns of glacier-wetland hydrological connectivity in the rapidly deglaciating Peruvian Andes. *Earth's Future*, *14*, e2026EF008149. https://doi.org/10.1029/2026EF008149

Received 16 JAN 2026
Accepted 1 JUN 2026

Author Contributions:

Conceptualization: D. Xuan, R. Becker, W. Buytaert
Data curation: D. Xuan
Formal analysis: D. Xuan, R. Becker
Funding acquisition: B. J. Davies, J. C. Ely
Methodology: D. Xuan, R. Becker, C. Onof
Resources: B. J. Davies, O. King, N. Montoya
Software: D. Xuan
Supervision: R. Becker, W. Buytaert

Abstract High-altitude wetlands are critical ecosystems that store water, regulate downstream flows, and sustain biodiversity. Their persistence is tightly linked to continuous water inputs from precipitation, groundwater, snow and glacier melt, making them highly vulnerable to climate-driven shifts in mountain hydrology. Rapid glacier retreat, altered precipitation regimes, and rising temperatures are transforming water availability across mountain regions worldwide, but their consequences for wetland stability remain poorly understood. Here, using high-resolution satellite-based mapping (2019–2025) and statistical analyses, we investigate the spatiotemporal dynamics and hydroclimatic drivers of high-altitude wetlands at two tropical Andean study sites in Peru: Cordillera Vilcanota and the La Raya. We demonstrate that precipitation-derived water is the primary driver of wetland seasonality, explaining up to 30% of the observed variability. This influence weakens in areas close to glaciers, where wetlands exhibit reduced seasonal fluctuations in surface wetting and drying, suggesting a local dampening effect of glacial runoff on wetland hydrological variability. Our spatially explicit analysis demonstrates that this dampening effect attenuates rapidly with distance and is no longer detectable beyond approx. 12 km from glaciers, indicating that the hydrological influence of glacier melt is highly localized and that most high-mountain wetlands are effectively decoupled from glacier-melt processes. The study highlights the critical role of glacier–wetland hydrological connectivity in the context of hydrological changes in mountain regions.

Plain Language Summary High-altitude wetlands are important and unique ecosystems in mountain regions. They store water, support diverse plants and animals, and regulate water availability further downstream. These wetlands depend on a steady water supply, which makes them sensitive to climate change. In many mountain regions, glaciers are shrinking, rainfall patterns are shifting, and temperatures are rising. These changes affect the amount of water available throughout the year, but it remains unclear how mountain wetlands respond. In this study, we examine how wetlands have changed over time in two areas of the Peruvian Andes: one with glaciers and another where glaciers have recently disappeared. Using satellite images from 2019 to 2025, we track monthly changes in wetland extent and analyze how climate and water availability influence wetland behavior. We find that water from rainfall is the main factor controlling whether wetlands become wetter or drier over time. Wetlands near glaciers change less throughout the year, likely because glacier melt provides a more stable water source. This stabilizing effect weakens rapidly with distance from glaciers and disappears beyond about 10 km, meaning most mountain wetlands are not influenced by glacier melt.

1. Introduction

Due to their strong dependence on consistent and sufficient water inputs, wetlands are highly sensitive ecosystems. This vulnerability is especially pronounced in high mountain regions, where rapid glacier retreat and changing precipitation and temperature regimes are causing significant changes in mountain hydrology (Huss & Hock, 2018). With mountain glacier extent and volume projected to continue decreasing throughout the 21st century (Marzeion et al., 2020; Radić et al., 2014; Zekollari et al., 2025; Zemp et al., 2015), the nature and spatiotemporal patterns of glacier melt input will change. In areas that are highly impacted by cryospheric changes, this may result in wetland degradation or loss and affect their ecosystem services (Haeberli &

Validation: D. Xuan, R. Becker, M. Vargas Valverde, B. J. Davies, O. King, N. Montoya, C. Onof, A. C. Ross, W. Buytaert
Visualization: D. Xuan, R. Becker
Writing – original draft: D. Xuan, R. Becker
Writing – review & editing: D. Xuan, R. Becker, M. Vargas Valverde, B. J. Davies, J. C. Ely, O. King, N. Montoya, C. Onof, A. C. Ross, W. Buytaert

Weingartner, 2020). A key question, therefore, is the extent to which the dynamics of high-mountain wetlands in close proximity to glaciers are influenced by glacier meltwater contributions, and by glacier loss.

There is no universally accepted definition of high-mountain wetlands. Here, we define them as permanently or seasonally saturated areas located typically above the climatic limits of forest growth, where present, and below the permanent snow line (Chatterjee et al., 2010). These wetlands typically develop in flat or gently sloping valley bottoms, over colluvial deposits and in infilled lakes (Davies et al., 2026; Emmer, 2024), where water can accumulate and create conditions that support year-round vegetation cover in otherwise harsh, rocky, and steep environments (Chimner et al., 2010; Maldonado, 2014). In the central Andes, they occur widely at elevations of 3,500–5,200 m a.s.l. (INAIGEM, 2023a) and are locally known as "bofedales." These bofedales are high-Andean peat-forming wetlands dominated by hydrophytic cushion plants, particularly Distichia muscoides (Maldonado-Fonkén et al., 2024; Oyague & Cooper, 2020). Their dense vegetation and peat soils slow the transit of water through the landscape and can create natural damming and isolated pools that regulate drainage and seasonal hydrological wetland-stream connectivity (Chimner et al., 2023; Oyague & Cooper, 2020; Wunderlich et al., 2023). While most high-Andean wetlands are located in valleys far and disconnected from glaciers, this study focuses specifically on wetlands located in close proximity to glaciers, where hydrological connectivity with glacier meltwater may influence wetland dynamics.

Depending on their topographical position and proximity to glaciers and snowfields, high-mountain wetlands may be sustained by varying contributions from precipitation, groundwater flow, snowmelt, and glacier runoff (Cooper et al., 2019; Gribbin et al., 2024; Ross et al., 2023), resulting in complex spatial patterns of their occurrences. The high variability in mountain temperature and precipitation further interacts with these fine-scale landscape features, producing highly heterogeneous environmental conditions that influence wetland persistence. Elevation, aspect, slope, and terrain complexity impact near-surface microclimates, leading to steep temperature gradients over short distances (Mountain Research Initiative EDW Working Group, 2015). Orographic uplift further enhances spatial precipitation variability, with windward slopes receiving substantially greater moisture inputs than leeward slopes (Rojas & Minder, 2024). Similarly, glacier melt processes depend on elevation, aspect, and slope, which generate strong spatial variation in melt rates and in the timing and magnitude of meltwater reaching downstream wetlands.

Due to this topographic and hydro-climatic complexity, the extent of hydrological connectivity between glaciers and mountain wetlands, and the subsequent impact of glaciological changes on wetlands is still unclear. While some studies have found no relationship between wetland and glacier melt dynamics (Cooper et al., 2019), others suggest that ongoing glacier retreat may initially drive wetland expansion, followed by a subsequent decline (Polk et al., 2017). Understanding hydrological connectivity between glaciers and wetlands is therefore key to assessing the impact of glacier retreat on mountain wetlands. Previous studies have addressed these questions using hydrogeological isotope analyses (Cooper et al., 2019; Gribbin et al., 2024) and local hydrological modeling studies (Ross et al., 2023). These methods require intensive data collection and data input, typically limiting their spatial coverage to single catchments and temporal resolution to short monitoring periods. Yet, due to the above mentioned topographic and hydro-climatic complexity in mountain regions, a longer-term and spatially explicit landscape-system perspective will enable the improved quantification of wetland–glacier connectivity and to predict how and most importantly, where ongoing hydro-climatic changes will alter wetland dynamics.

We hypothesize that wetlands located close to glaciers are hydrologically connected to glacier meltwater through surface and groundwater pathways, and that this connection influences inter- and intra-annual variability in wetland moisture conditions. In such connected systems, reductions in glacier meltwater supply may therefore increase the risk of seasonal drying, although we do not expect complete wetland loss as precipitation reveals to remain a dominant driver, even near glaciers.

To test this hypothesis and to bridge the gap between local- and landscape-system scale analyses, we use an unprecedented 6-year time series of satellite-derived wetland observations to capture spatio-temporal wetland dynamics. We couple these observations with a spatially distributed regression analysis to identify the dominant drivers of wetland seasonality. Although this method does not allow direct identification of water source origins or subsurface flow pathways, it provides valuable insights into wetland behaviors at landscape scale.

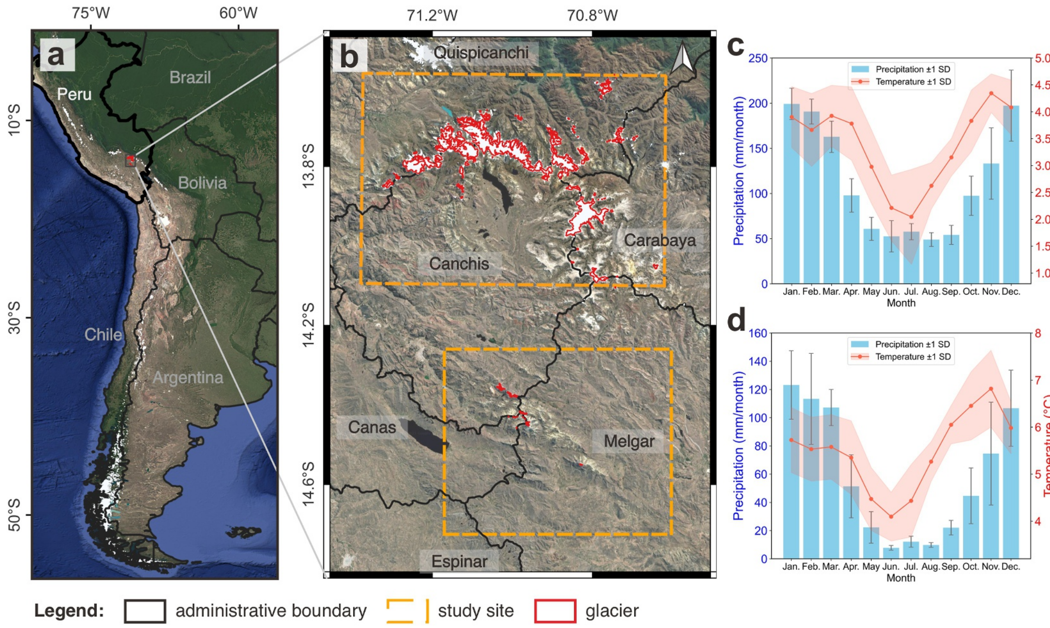

Figure 1. Location and climatic background of the two study sites. (a) Overview of the Andes and neighboring countries. (b) Enlarged view of the two study sites: the Cordillera Vilcanota in the north and La Raya in the south. Glacier outlines are from the Randolph Glacier Inventory (RGI) Version 7.0 (RGI Consortium, 2023), representing conditions around the year 2000. (c and d) Mean monthly precipitation and air temperature from January 2019 to February 2025 (the study period) for the Cordillera Vilcanota (c) and the La Raya region (d). Precipitation was derived from the hourly IMERG product (Huffman et al., 2014), while air temperature at 2 m above the surface was obtained from the monthly averaged ERA5-Land data set (Muñoz-Sabater et al., 2021).

2. Methods and Data

2.1. Study Sites

We focus our analysis on two high-altitude study sites in Southern Peru to test our hypothesis (Figures 1a and 1b). Both sites are experiencing rapid glacio-hydrological changes, driven by ongoing climate warming. While the Cordillera Vilcanota (Figure 1b, north) continues to host substantial glacier coverage (approx. 5.4% in our study site), the La Raya region (Figure 1b, south) has become largely ice-free in the past decades (glacier coverage <0.1%). The two study sites are located in close proximity to each other, in a semi-arid High-Andean mountain landscape, around 3,300–6,000 m a.s.l.. Approximately 4%–5% of both study sites are covered by wetlands, fed by rainfall, groundwater, and/or glacier melt. A strong precipitation seasonality, with a wet season from October to April and a dry season from May to September (Figures 1c and 1d), drives a pronounced seasonal drying–wetting dynamic of wetlands (Gribbin et al., 2024; Ross et al., 2023).

The northern site encompasses a domain of 4,500 km^2 around the Cordillera Vilcanota (71°W, 13.7°S), the most extensive glacierized mountain range in the South of Peru and home to one of the world's largest tropical ice caps, the Quelccaya ice cap. Altitudes range from 3,260 to 6,030 m a.s.l.. Mean annual precipitation rates during our study period (2019–2025) are approx. 1420 mm/year. Mean monthly temperature variations are low and vary between 1.7°C and 4.5°C (Figure 1c), with colder temperatures during the dry season. Glaciers and the Quelccaya ice cap are rapidly shrinking (Taylor et al., 2022) and in the past six decades (1962–2020) the Cordillera Vilcanota has lost approx. 51% of its glacier coverage (INAIGEM, 2023b). The region's rapid glacier retreat makes it well suited for investigating meltwater effects on wetland dynamics and glacier–wetland hydrological connectivity.

Our southern study site is located approx. 60 km south of the Cordillera Vilcanota (71°W, 14.3°S) and spans a region of 3,100 km^2 around the La Raya mountain range, at altitudes between 3,880 and 5,270 m a.s.l.. This region has a more centered position on the Andean plateau and receives less precipitation than our northern site due to its larger distance and leeward position with respect to the prevailing advective moisture transport from the Amazon Basin (Drenkhan et al., 2015). Annual precipitation rates reach on average 713 mm/year. Mean monthly temperatures vary between 3.8°C and 6.9°C (Figure 1d). The Randolph Glacier Inventory, which has an approximate date of 2000, suggests the existence of small ice bodies at high elevations here (outlines shown in Figure 1b), but more contemporary satellite images show that the region has lost nearly the entirety of its glacier coverage, leaving many formerly ice-covered mountain tops and adjacent catchments ice free. We selected this site to investigate wetland hydrology in a post-glacial landscape, where past hydrological connectivity between glaciers and wetlands may have existed but has been disconnected by continued glacier retreat.

2.2. Quantifying Temporal and Spatial Wetland Extents

We mapped wetlands and their temporal dynamics using monthly satellite imagery from January 2019 to February 2025, building on the approach of Becker et al. (2026). Spectral, topographic, and ecological data were compiled from Sentinel-1 and Sentinel-2 imagery, the 30-m NASA SRTM DEM, and the RESOLVE ecoregions (Dinerstein et al., 2017). Within defined training areas, we extracted random samples to derive predictor variables including surface-moisture indices, vegetation indices, as well as topographic and ecological metrics (Text S1 in Supporting Information S1). These predictors informed a Random Forest classifier, which we used to map high-altitude wetlands. With this approach we achieved an average mapping accuracy of 91% (±1%) when validated against an existing wetland data set (INAIGEM, 2023a). Monthly wetland extents were generated by repeating the classification for monthly image subsets. To address data gaps from cloud cover in the wet season, we applied a 3-month rolling window, to build 3-monthly image composites and assigned the resulting average extent to the central month. To analyze spatial patterns in wetland dynamics, we delineated sub-catchments from the SRTM DEM using a 5,000-pixel contributing-area threshold and quantified monthly wetland area within each unit (See Text S1 and S2 in Supporting Information S1 for details on the mapping approach and thresholding).

2.3. Gridded Precipitation and Temperature Data

Monthly precipitation data were obtained from the hourly IMERG product, a satellite-based precipitation estimate from NASA's GPM mission (Huffman et al., 2014), with a spatial resolution of $0.1° \times 0.1°$. This data set, despite its coarse resolution, is sufficient to capture precipitation variations across altitudes in our study sites (Text S3 in Supporting Information S1). For the regression analysis, monthly precipitation totals were extracted at the centroid of each sub-catchment, to match the spatial unit of the wetland analysis. Air temperature at 2 m above the surface was obtained from the monthly averaged ERA5-Land data set (Muñoz-Sabater et al., 2021), at a resolution of $0.1° \times 0.1°$. Similarly to the precipitation data extraction, we extracted the mean monthly temperature value for each sub-catchment at its respective centroid, to account for spatial temperature variations.

2.4. Glacier-Dilution Algorithm and Distance Group Classification

In the absence of spatially distributed observations of glacier meltwater, we developed an algorithm to approximate the downstream attenuation of meltwater influence within the river network. Based on the Strahler stream order (Strahler, 1957) and flow accumulation, we ranked single stream segments of the river network. Glacier-proximal segments were assigned a maximum meltwater signal. This signal was progressively diluted at each stream confluence as non–glacier-fed tributaries entered the network, producing a continuous index of relative glacier influence for each stream segment (see detailed methodology in Text S4 and Figure S4 in Supporting Information S1). Each sub-catchment was then assigned the index of its longest intersecting stream segment. Subsequently, the sub-catchments were grouped into the three classes "close," "medium," and "far," indicating not only the distance to glaciers but also the potential glacier melt influence in each of the sub-catchment's main stream. The glacial impact propagation maps and the distributions of glacial impact categories for the two study sites are presented in Figure 2.

In the glacierized Cordillera Vilcanota, the three categories "close," "medium," and "far" from glaciers and glacial impact, reflect present-day conditions as glaciers are still present and abundant. In the La Raya, where current glacier extent is minimal, the same classification was applied using the glacier outlines from the year 2000 (Pfeffer et al., 2014). Here, the three categories refer to potential former distances and strengths of glacier melt impacts. Using the same classification approach in both regions allows a direct comparison of wetland dynamics across equivalent distance–influenced classes. This enables us to distinguish effects attributable to glacier meltwater from those arising from other factors such as topography or climatic drivers. Although hydrological connectivity between glacier-fed streams and wetlands are still debated and wetlands may be decoupled from

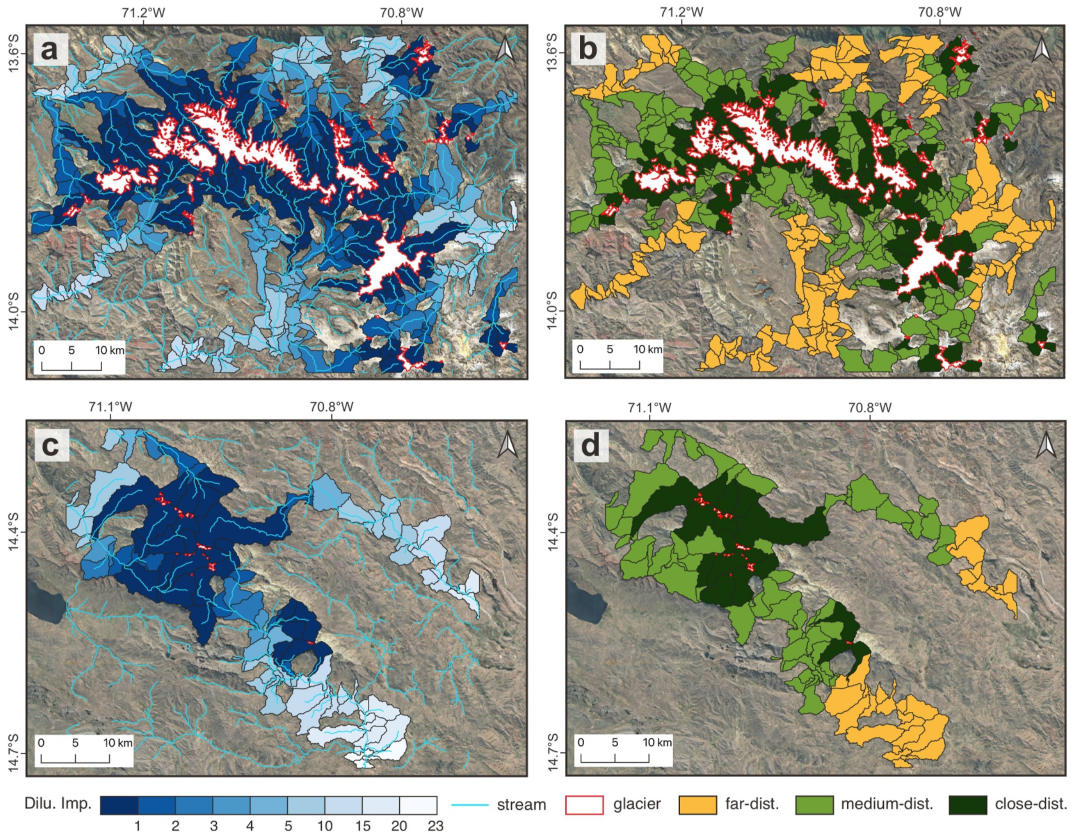

Figure 2. Glacial impact propagation maps and the associated three distance groups in the Cordillera Vilcanota (a–b) and La Raya (c–d) glacier dilution with stream networks (a, c) and distance groups (b, d).

streamflow (Cooper et al., 2019; Gribbin et al., 2024), our approach still provides a useful proxy for relative meltwater influence. By following the stream network, the glacier melt influence does not rely on distance alone, but it implicitly incorporates the effects of topography and drainage pathways. This makes it a more hydrologically informed indicator of potential meltwater contributions than a simple distance-based metric.

2.5. Multiple Linear Regression Analysis

Multiple linear regression analysis was applied to identify the main hydro-climatic drivers (predictor variables) of wetland dynamics (the response variable) and to quantify their independent contributions. Predictor variables included monthly average temperature and precipitation, as well as seasonality and long-term trends. The general form of the regression equation is given below:

$$\tilde{Y} = \alpha_0 + \sum_{i=1}^{n} \alpha_i \widetilde{X}_i \tag{1}$$

All variables (Y and X_i) were standardized prior to regression as $\tilde{Z} = \left(Z - \bar{Z}\right)/\sigma_Z$, where Z represents either Y or any X_i; $\bar{Z}$ is the mean of the original variable Z; and σ_Z is its standard-deviation (SD). $\tilde{Y}$ is then the standardized dependent variable; $\widetilde{X}_i$ is the standardize predictor for sub-catchment i; α_i is its regression coefficient and α_0 is the intercept term.

To explicitly account for the strong seasonal cycle, we included seasonality indicators as predictor variables to improve our model accuracy by isolating recurring seasonal patterns. For this, each month was mapped onto a unit circle, and the sine and cosine of the month were used as predictors instead of raw numerical values (January = 1, …, December = 12), thereby avoiding undue emphasis on December and ensuring a continuous

10.1029/2026EF008149

Table 1
Standard Deviation (SD) of Each Variable

Study site	Predictors				Response
	temp. (°C)	precip. (mm)	seasonal. (−)	trend (months)	wetland (km^2)
Cord. Vilcanota	1.92	76.58	0.71	21.36	0.35
La Raya	1.57	42.68	0.71	21.36	0.84

Note. For temperature (temp.), precipitation (precip.), trend, and wetland area, the SD is calculated directly from the data. For seasonality (seasonal.), the SD is theoretical: $1/\sqrt{2} \approx 0.71$, derived from the sine and cosine components of the month over a full annual cycle.

representation of seasonality. For subsequent analyses, the amplitude of the seasonal cycle (S) was derived from the sine and cosine components as

$$S = \sqrt{\alpha_{\text{sin}}^2 + \alpha_{\text{cos}}^2} \tag{2}$$

which represents the combined magnitude (Euclidean length) of the standardized regression coefficients α_{sin} and α_{cos}. The trend indicator is defined as a time-ascending index, ranging from 1 (as January 2019) to 74 (as February 2025).

As several predictors exhibit strong intercorrelations, Ridge regression was applied to mitigate the effects of multicollinearity. Ridge regression introduces an L2 regularization term to the loss function, penalizing large coefficient values and allowing correlated predictors to share explanatory power more evenly (McDonald, 2009). The Ridge estimator $\hat{\alpha}$ is obtained by minimizing the residual sum of squares (RSS) plus an L2 penalty term (Marquardt & Snee, 1975), as expressed in Equation 3. The optimal set of coefficients was selected by cross-validation (80% training, 20% testing) based on achieving a higher determination coefficient ($R^2 > 0.7$) and a lower normalized root-mean-square error (NRMSE < 0.2).

$$\hat{\alpha} = \arg\min_{\alpha} \left\{ \underbrace{\sum_{i=1}^{n} \left(y_i - \mathbf{x}_\mathbf{i}^{\mathbf{T}}\alpha\right)^2}_{\text{RSS}} + \underbrace{\lambda \sum_{j=1}^{p} a_j^2}_{\text{L2 penalty term}} \right\} \tag{3}$$

In Equation 3, $\hat{\alpha}$ denotes the estimated coefficient vector under the Ridge penalty, where $\alpha = (\alpha_1, \ldots, \alpha_p)^{\mathrm{T}}$ represents the regression coefficients to be estimated. y_i is the response variable for sub-catchment i, $\mathbf{x}_i = (x_{i1}, \ldots, x_{ip})^{\mathrm{T}}$ is the predictor vector for sub-catchment i, n is the number of sub-catchments, p is the number of predictors, and $\lambda \geq 0$ is the regularization parameter. As λ increases, the coefficients are increasingly shrunk toward zero.

Following the Z-score transformation described in Equation 1, all predictors ($\widetilde{X}_i$) and the response variable ($\tilde{Y}$) were standardized using the mean and SD calculated from the full study-area data set, rather than from individual sub-catchments. This approach preserves inter-catchment variability and allows direct comparison of coefficient magnitudes spatially. Table 1 summarizes the 1-SD values for each predictor and the wetland response variable at both study sites. A coefficient of 2 represents that a 1–SD increase in a predictor corresponds to a 2–SD increase in the response. For example, in the Cordillera Vilcanota region, this translates to a physical change of $2 \times 0.35 = 0.7$ km^2 in wetland area (Table 1). Larger coefficients therefore reflect stronger effects, allowing the importance of predictors to be directly ranked and compared by their coefficient magnitudes. Unlike temperature and precipitation, which reflect the driving mechanisms of wetland dynamics and carry the physical meanings of a 1-SD change, the seasonality and trend predictors are used to explicitly characterize the seasonal patterns and long-term trends of wetlands, as well as to account for the shared seasonality and trends within the climatic predictors. A 1-SD change of 0.71 in the seasonal predictor corresponds to approximately 71% of the full seasonal amplitude, representing a moderately strong seasonal shift, whereas a 1-SD change in the trend predictor simply reflects the length of time series.

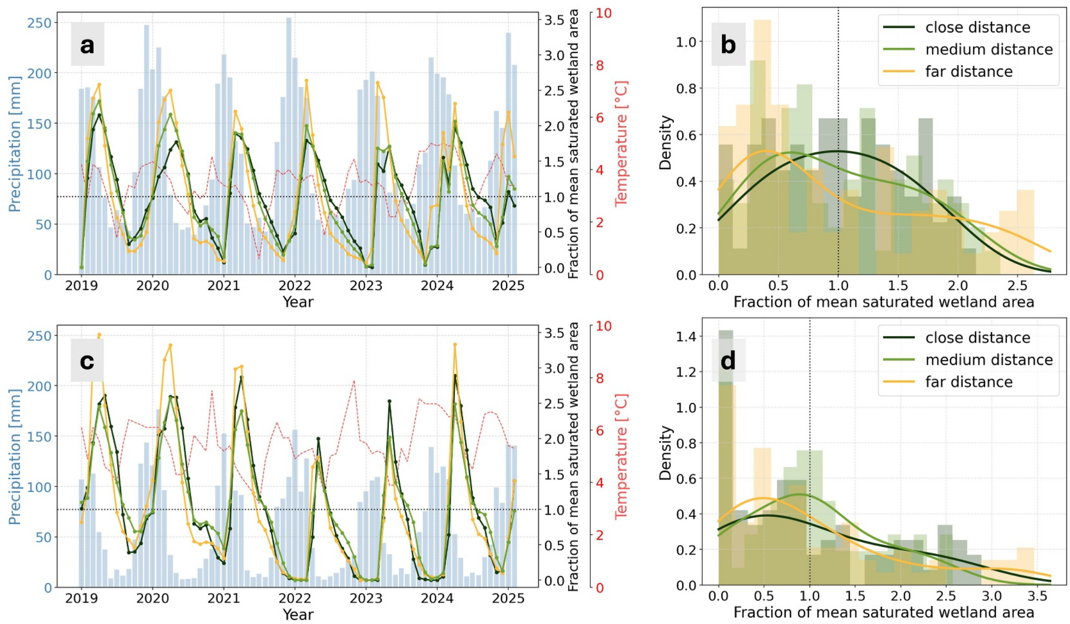

Figure 3. Seasonal wetland wetting and drying dynamics around the Cordillera Vilcanota (a, b) and around the La Raya range (c, d) in close, medium and far distances from (formerly) glacierized areas. Saturated wetland area is expressed as a fraction of its multi-annual average. For example, a value of 2.0 shows a doubling (=200%) of the average saturated wetland area.

We applied a cross-Spearman correlation analysis to identify the most significant time lag between the wetland series and the climatic predictors (Text S5 in Supporting Information S1). This analysis showed that a 3-month lag resulted in the strongest and most significant relationship in the Cordillera Vilcanota. For consistency and direct comparison, we adopted the same lag for the southern site. Based on these correlation results, we applied 3-month time lag to temperature and precipitation in all regression models to best capture the wetland response to climatic variability. Separate regression models were constructed for each sub-catchment at the two study sites to assess the spatially distributed effects of climatic drivers on wetland dynamics and to evaluate how glacial presence modulates these effects. We then performed 500 bootstrap resampling iterations to assess the robustness of each regression coefficient. Only statistically significant values were retained. For each distance group, the mean, standard error, and corresponding 95% confidence intervals of these significant coefficient samples were then calculated based on the Student's *t*-distribution.

3. Results and Discussion

3.1. Seasonality of Wetlands

In both study regions, wetlands show pronounced temporal variability that reflects the strong seasonality of precipitation. Saturated wetland area increases during the wet season and decreases during the dry season, with a characteristic 3-month lag between peak rainfall and the maximum extent of saturation (Figures 3a and 3c). This delay likely reflects two hydrological and ecological processes: (a) the time required for rainfall to infiltrate, recharge groundwater, and subsequently supply wetlands through hillslope discharge (Cooper et al., 2019; Gribbin et al., 2024; Ross et al., 2023); and (b) the delayed onset of vegetation greening following the start of the rainy season, which is captured by our remote-sensing–based wetland detection that is particularly sensitive to photosynthetically active, green surface features (Dangles et al., 2017). Across all three glacier–distance classes (close, medium, far), wetlands show the same precipitation response time, reinforcing the conclusion that precipitation is the dominant driver of seasonal wetland dynamics, even in glacier–proximal areas. Field-based studies such as Oyague et al. (2022), demonstrate that this seasonal variability in Andean wetlands is not limited to surface wetting and drying but is also shown in vertical fluctuations of the groundwater table, driven by precipitation and by topographic gradients. Such studies provide detailed insights into subsurface flow paths and water table dynamics at local scales. In the following, our remote-sensing approach focuses on the detection of

Table 2
The Average Explained Variance (%) and Its Corresponding 95% Confidence Intervals (CI) for Each Predictor Across Distance Groups at Two Study Sites

		Variables			
Study site	Distance to glaciers	Precipitation	Temperature	Seasonality	Trend
Cordillera Vilcanota	far dist.	24.0 ± 1.7	2.2 ± 6.1	37.2 ± 2.1	7.1 ± 1.1
	medium dist.	23.0 ± 1.3	5.0 ± 1.6	35.8 ± 1.4	7.2 ± 0.7
	close dist.	21.9 ± 2.1	4.1 ± 2.5	37.1 ± 2.6	8.3 ± 1.9
La Raya	far dist.	29.5 ± 3.6	/	20.4 ± 2.5	6.7 ± 0.7
	medium dist.	22.1 ± 1.5	/	31.6 ± 3.8	6.7 ± 0.9
	close dist.	23.9 ± 2.6	/	33.7 ± 3.8	5.9 ± 1.9

spatial patterns of these processes at the land surface, which allows us to identify hydrological connectivity at landscape-scales.

Our remote sensing-based analysis shows, that despite this strong precipitation-driven pattern, clear spatial differences can be observed. In the still-glacierized Cordillera Vilcanota, sub-catchments close to glaciers display a reduced seasonal amplitude in wetland wetting and drying extent (Figure 3a) and a uni-modal distribution (Figure 3b), indicating more stable year-round wet conditions. In contrast, sub-catchments far from glaciers show the largest seasonal wetland fluctuations and a distinct bimodal distribution, reflecting pronounced wetting and drying cycles. Wetlands at intermediate distances exhibit transitional behavior. These patterns suggest that glacier meltwater exerts a buffering effect on wetland variability, stabilizing wetland extents in glacier-proximal areas. This effect however diminishes rapidly and is no longer detectable in the far-distance class.

In the La Raya range, where current glacier meltwater inputs are minimal or absent, wetland dynamics do not differ between sub-catchments close to or far from formerly glaciated areas (Figures 3c and 3d). Inter-annual variability in saturated wetland area is substantially larger than in the Cordillera Vilcanota (CV = 0.75 vs. 0.54), and wetlands frequently dry out during the dry season (e.g., in 2022–2024). These observations point to a strong dependency on seasonal precipitation and the absence of a stabilizing influence from glacier meltwater.

3.2. Hydro-Climatic Drivers of Wetland Dynamics

3.2.1. Precipitation

The results from our regression analysis confirm that precipitation is the dominant driver of wetland saturation in both study sites. This influence likely occurs both through direct precipitation inputs to wetlands and through the recharge and saturation of hillslope aquifers and shallow groundwater systems that subsequently feed wetland areas. Precipitation lagged by 3 months, explains approx. 22%–24% and 22%–30% of the variability of saturated wetland areas in the Cordillera Vilcanota and the La Raya mountain ranges, respectively (Table 2, see detailed calculation in Text S6 in Supporting Information S1).

In the glaciated Cordillera Vilcanota, precipitation plays a stronger role in sub-catchments located farther from glaciers (yellow lines), which also tend to exhibit higher seasonal variations (Figure 4a), underlining our results presented above. Wetland sensitivity to precipitation increases with distance from glaciers, with average co-efficients rising from 0.14 (±0.05) in glacier-proximal areas to 0.26 (±0.09) farther away (Figure 4a). In the southern and northwestern parts of the region, precipitation coefficients commonly exceed 0.5, and in some cases 2.0, indicating particularly strong precipitation control (Figure 5a). Some regions in the northeastern and southwestern parts of this study site do not follow this pattern, but here precipitation–wetland relationships are statistically insignificant and therefore less reliable. A 1–SD increase in precipitation (≈76.58 mm per month; Table 1) increases wetland wetted area by up to 0.12 km^2 in distant sub-catchments, which corresponds to roughly four times the response observed in glacier–proximal ones. Similarly, a 1–SD (0.71; Table 1) increase in sea-sonality corresponds to an increase of approximately 0.12 km^2 in the more distant sub-catchments, but only about

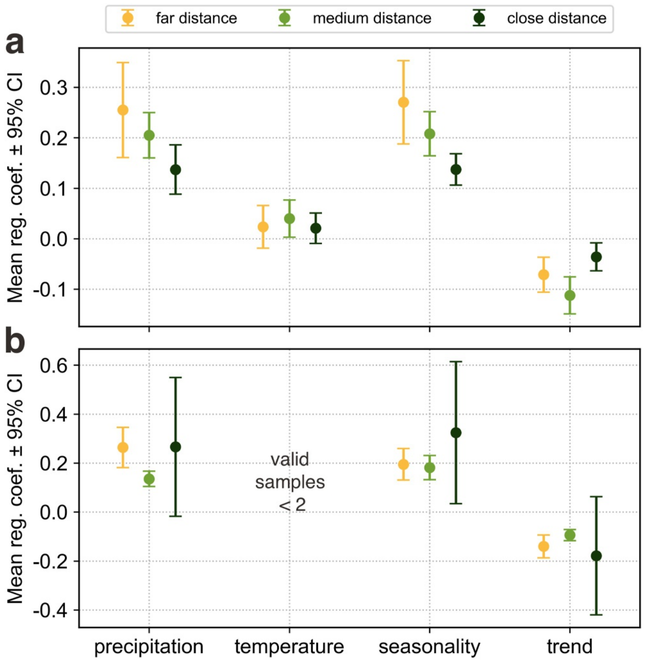

Figure 4. The average value of significant regression coefficients (reg. coef.) and its related 95% confidence interval (CI) across the three distance classes in Cordillera vilcanota (a) and in the La Raya (b). Precipitation, temperature, and trend were predictive variables in the Ridge regression, while seasonality was derived from α_{sin} and α_{cos}. The detailed values are shown in Table S2 and Text S7 in Supporting Information S1.

0.04 km^2 in glacier–proximal ones. This indicates that wetlands distant from glacier influence are roughly three times more sensitive to seasonal variability than those nearby.

In the La Raya region, these distinct spatial variations in precipitation influence and seasonality across the distance groups are not apparent (Figure 4b) and the effect of precipitation becomes more spatially heterogeneous (Figure 5b). No clear distinction is observed between the far- and close-distance classes, both showing average coefficients of around 0.26. Within the close-distance group, the effects of precipitation and seasonality become markedly less stable, with the 95% confidence interval expanding by a factor of six for precipitation and 10 for seasonality. Although average precipitation coefficients in the far-distance groups are similar between regions (≈0.26), the corresponding wetland response differs. In the La Raya region, a 1–SD increase in precipitation (≈42.68 mm per month; Table 1)—about 56% of the SD in the Cordillera Vilcanota—results in 2.4 times greater saturated wetland area. This indicates a proportionally stronger dependence on precipitation in the deglaciated La Raya landscape. These patterns align with our earlier findings, indicating once more that precipitation dominates wetland drying and wetting.

The spatially distributed results at sub-catchment level (Figures 5a and 5b) further indicate that both rainfall amount and relative wetland extent per sub-catchment (Figure S5 and Text S8 in Supporting Information S1) modulate wetland sensitivity to precipitation variability. In the north-eastern Cordillera Vilcanota, located on the windward slope facing the Amazon basin, mean precipitation is higher but the relationship between rainfall and wetland dynamics is weak or statistically insignificant. In contrast, in the drier La Raya mountain range, wetlands show a stronger precipitation dependency and a more pronounced intra- and inter-annual variability.

Overall, the strong control of precipitation on wetland dynamics is consistent with previous research, which shows that high-Andean wetlands are primarily sustained by direct precipitation and hillslope groundwater discharge recharged by rainfall (Cooper et al., 2019; de la Fuente et al., 2021; Gribbin et al., 2024). Isotope evidence from Cooper et al. (2019) shows that wetland hydrology in the high central Andes remains largely independent of glacier runoff, with meltwater bypassing wetlands via stream channels. This assumption, that wetland and glacier dynamics represent two separate systems, would explain the strong seasonal drying and wetting of wetlands in response to rainfall, even in sub-catchments with potentially high glacier melt contribution. It also explains the persistence of wetlands and their maintained seasonality in the La Raya mountain region, where glaciers have already disappeared in most sub-catchments, and where precipitation is the only remaining water source (Figure 3c).

3.2.2. Temperature

Temperature effects are generally weak across both study sites (Figures 5c and 5d). Most sub-catchments show statistically insignificant relationships with temperature, and no distance-dependent pattern emerges. Temperature coefficients are consistently smaller than precipitation coefficients. A 1–SD increase in temperature in the Cordillera Vilcanota (corresponding to around 2°C; Table 1) results in a standardized wetland response ranging from −0.01 to 0.07 SD (corresponding to −0.008 km^2 to +0.06 km^2). The effect of temperature in the La Raya range is generally statistically insignificant.

In the Cordillera Vilcanota, average coefficients are similar across distance groups (0.03 ± 0.04), yet individual sub-catchments display contrasting responses. Some glacier–proximal sub-catchments show negative coefficients (<−0.1), suggesting drying with higher temperatures, while others exhibit positive coefficients (>0.1), indicating a wetting effect (Figure 5c). Similar inconsistencies also occur in sub-catchments farther from glaciers and within the La Raya range (Figure 5d). These opposing local responses, combined with predominantly

10.1029/2026EF008149

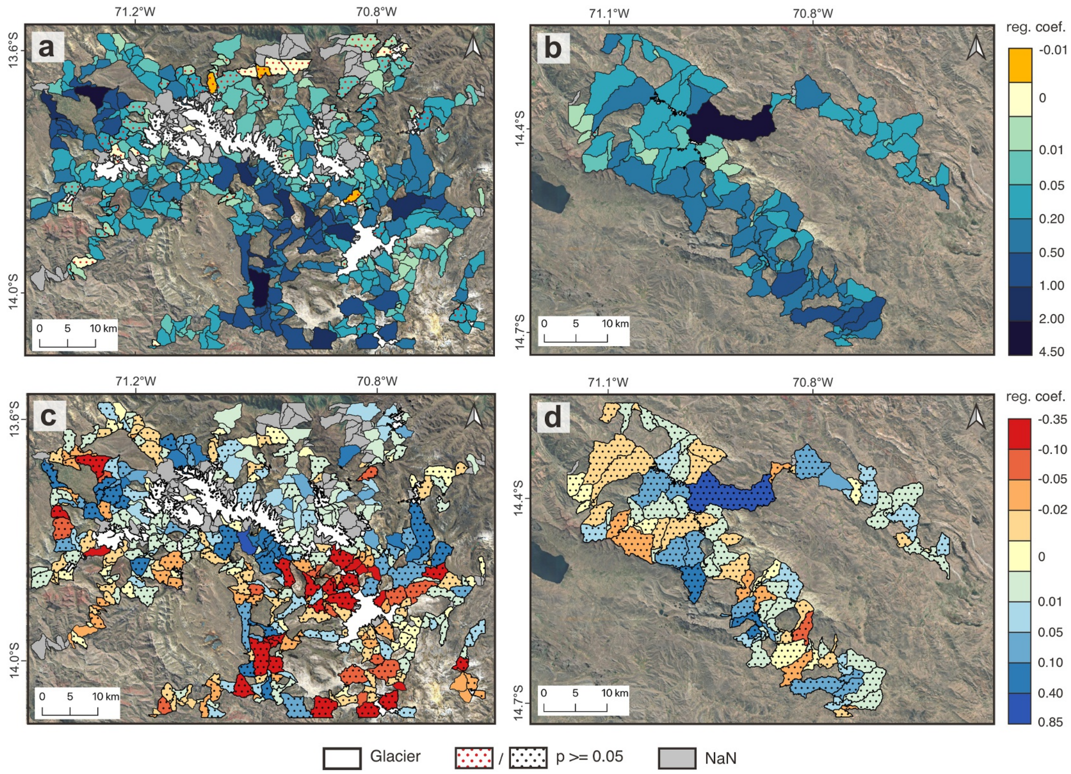

Figure 5. Ridge regression coefficients for precipitation (a–b) and temperature (c–d) across three distance classes in each sub-catchment at both study sites: (a, c) the Cordillera Vilcanota; (b, d) the La Raya range.

insignificant coefficients, suggest that temperature effects are highly variable and should be interpreted with caution.

Overall, these results are contrary to our expectations. A stronger positive temperature–wetland relationship might be expected in glacier–proximal areas of the Cordillera Vilcanota if warmer periods enhanced meltwater inputs. The absence of such a pattern suggests that the relatively small seasonal temperature range (1.7–4.5°C) does not substantially increase glacier meltwater contributions. This is also confirmed by Fyffe et al. (2021), who found that rather than temperatures, intense radiative fluxes and their surface albedo are the primary drivers of glacier melt in this region, which can result in ablation in low temperatures. In the La Raya mountains, where glacier cover is minimal (0.1%) and temperature variability is similarly limited (3.8–6.9°C), temperature changes and glacier areas are likely insufficient to generate additional meltwater to influence wetland extents.

The limited role of temperature may also partly reflect the nature of our regression approach, which attributes most of the explained variability to the dominant precipitation signal. This does not imply that temperature effects are absent. Rather, their relative contribution is small and therefore masked by stronger precipitation-driven dynamics. Furthermore, we only consider monthly temperature variations, in a region where daily temperature and radiation fluctuations are high and can cause significant variations in glacier melt runoff. In addition, the chosen 6-year time period is too short to show any long-term temperature trends, which could impact long-term wetland dynamics.

3.2.3. Glacier Melt

While our analysis does not allow direct quantification of glacier melt contributions, several independent results support our hypothesis, that wetlands located close to glaciers are hydrologically connected to glacier melt. A key result is the decline in the regression coefficients of precipitation and seasonality toward glacier–proximal areas (precipitation: 0.26 → 0.14; seasonality: 0.27 → 0.14; Figure 4a). This reduced precipitation importance indicates that additional water sources, such as glacier melt, gain influence near glaciers and help buffer seasonal wetland variations. This interpretation aligns with isotope evidence from Gribbin et al. (2024), who detected a small but

Table 3
Summary of Sub-Catchment Distances to the 2000 Glacier Outlines Across Distance Groups Using Trimmed Means and 5th–95th Percentile Statistics in Both Study Sites

	Cordillera Vilcanota			La Raya		
	p5 (km)	mean (km)	p95 (km)	p5 (km)	mean (km)	p95 (km)
close dist.	1.3	2.8	4.9	2.8	6.0	12.3
medium dist.	2.0	5.0	10.3	3.6	10.0	22.1
far dist.	5.6	11.7	21.6	7.9	17.9	25.7

measurable glacier-melt contribution to wetland waters in a glaciated catchment in the Cordillera Vilcanota. The buffering effect however is highly localized and detectable within approx. 2.8 km of glacier margins, already weakened by approx. 5 km, and dominated by precipitation beyond approx. 12 km (Table 3). This aligns with the observation that saturated wetland area shows a unimodal distribution in close proximity to glaciers, indicating higher wetland stability, while wetlands in farther distance to glaciers and in our deglaciated site, indicate a clear bi-modal wetting–drying seasonality (Figures 3b and 3c). Consistent with previous work (Buytaert et al., 2017), glacier-melt impacts thus diminish rapidly downstream. The absence of this distance-dependent pattern in the largely deglaciated La Raya region (Figure 4b) further supports our hypothesis. Here, wetland dynamics are even stronger driven by precipitation (average coefficient 0.27 ± 0.30 vs. 0.14 ± 0.05 in the Cordillera Vilcanota), reflected in faster dry-season wetland drying and occasional full desiccation (Figure 3c).

Hence, our spatially resolved analysis reveals systematic distance-related patterns that refine the previously stated assumption, that wetlands and glaciers represent two separate hydrological systems. We argue that although glacier-fed streams and wetlands may appear disconnected when examined at broader catchment extents, localized hydrological linkages still occur in glacier-proximal environments. The apparent discrepancy with earlier studies (Cooper et al., 2019) likely reflects scale effects. While glacier melt may influence wetlands at very short distances, this signal diminishes rapidly along the drainage network and becomes undetectable even at modestly larger spatial scales.

We note that our interpretation of spatial patterns in wetland dynamics relies on glacier proximity and stream networks, but does not fully account for the complex geomorphological context of high mountain wetlands. Wetlands in high mountain regions are located in very complex geomorphological environments that include a variety of glacial and Quaternary landforms, such as moraines, glacial lakes, kettle lakes, and tallus or debris deposits (Chesnokova et al., 2020; Glas et al., 2018), which shape hydrological pathways and control the occurrence of varying wetland types. These landforms often host aquifers of high permeability and storage capacities (Emmer, 2024; Ó Dochartaigh et al., 2019), which might contribute to the buffered seasonality as additional water stores and add to the spatial complexity of wetland types and their distinct wetting and drying dynamics. Our remote-sensing–based approach cannot separate their contribution from glacier melt effects. However, the fact that the buffering signal is only observed in the glacierized Cordillera Vilcanota study site suggests that these stores might be at least partly glacier-fed. In the La Raya mountain range similar peri-glacial landforms and hence, potential alternative water stores exist, but they do not exhibit the same buffering effect.

In conclusion, our spatially distributed analysis shows that glacier melt contributes measurably to wetland hydrology, but that this influence remains localized and does not extend beyond a few kilometers from glacier margins (≈1–5 km in the Cordillera Vilcanota). These are areas where riparian wetlands and wetlands associated with periglacial landforms dominate (Davies et al., 2026). Beyond this distance, precipitation and likely precipitation-recharged groundwater dominate wetland variability, consistent across both glacierized and deglaciated catchments. The rapid downstream attenuation of glacier influence explains why glacier–wetland linkages are not detected at broader catchment scales. The strong precipitation dominance makes wetlands more susceptible to pronounced intra- and interannual fluctuations, leading to higher annual wetting–drying amplitudes in disconnected glacier-wetland systems (Figure 6). Overall, these findings are supported by previous studies which show that while glacier melt can strongly influence hydrology close to glacier margins, this influence typically decreases within a few kilometers downstream as precipitation, groundwater recharge, and catchment storage processes increasingly dominate wetland and streamflow dynamics (Baraer et al., 2012; Buytaert et al., 2017; Mark & Mckenzie, 2007). Furthermore, even though wetlands and glacier-fed streams might

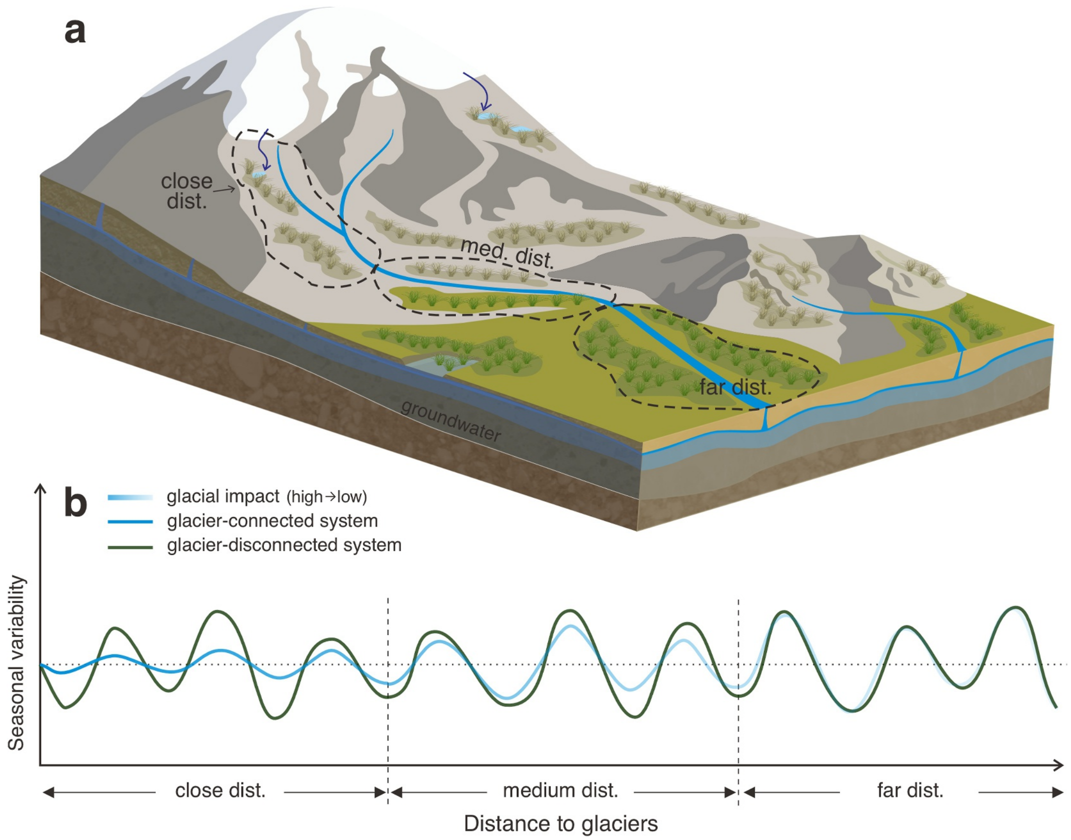

Figure 6. Conceptual model of high-Andean wetlands across the three distance classes (a) and the seasonality variability in glacier-connected and -disconnected wetland systems (b). The impact of glaciers on wetland seasonality is reduced in glacier-connected systems when the wetland is located far away, as indicated by the diluted blue color.

be disconnected, recent isotope work shows that groundwater-fed wetlands near glaciers can still contain a small but detectable glacier meltwater signal (Gribbin et al., 2024), suggesting that parts of the groundwater system receive glacier meltwater through infiltration. This indicates that glacier–wetland connectivity may occur indirectly via groundwater pathways rather than through surface streams.

3.3. Limitations and Uncertainties

The regression analysis considers a constant 3-month time lag between wetland dynamics and environment drivers for all sub-catchments. While this time lag correctly reflects the catchment-scale and distance-class response, wetland response to precipitation and temperature may vary between sub-catchments depending on topography and runoff pathways. Furthermore, snow processes are simplified in our analysis. While snow is included in total precipitation, we do not explicitly separate snowmelt from rainfall or account for melt timing. In our high Andean sites, rapid melt, limited snow pack and the prevalence of sublimation justify this assumption (Fyffe et al., 2021), though short-term meltwater contributions may be underestimated. In addition to climatic controls, human management practices such as irrigation can substantially alter high-Andean wetland dynamics. In the Peruvian Andes, irrigation of wetlands allows some wetlands to remain green during the dry season (Buytaert et al., 2006; Monge-Salazar et al., 2022; Verzijl & Quispe, 2013), leading our satellite-based approach to classify them as permanently wet despite underlying seasonality. This can bias estimates of wetting–drying cycles and the inferred role of glacier melt. Hence, part of the observed dampened wetland variability may reflect human intervention rather than natural hydro-climatic drivers. We furthermore acknowledge that the 30 m spatial resolution of the wetland maps, from which the monthly wetland dynamics are derived, might miss fine-scale hydrological or groundwater table variability. The derived signals represent surface wetness conditions, which we interpret as proxies for shallow groundwater and surface water presence. Accordingly, the results reflect landscape-scale wetness dynamics rather than detailed water table fluctuations. Finally, our assessment is based on only two study areas. Although these two sites contrast clearly the difference between wetlands in glaciated and deglaciated landscapes, regional variability may exist. Broader analyses at larger scale and at high spatial resolution are therefore needed to capture the full range of Andean glacier–wetland connectivity.

4. Conclusions

Using 6 years of high-resolution wetland maps and spatially distributed regression analysis, we demonstrate that glacier–wetland connectivity can influence wetland dynamics in still glacierized mountain regions, in southern Peru. Although precipitation dominates wetland variability in our glacierized as well as in our largely deglaciated study sites, a strong spatial gradient emerges in areas that receive meltwater inputs. Wetlands situated in close proximity to glacier margins show a reduced seasonality, indicating persistent water availability throughout the year. This pattern suggests that glacier meltwater is dampening the magnitude of wetting–drying cycles that would otherwise be driven by precipitation alone. Sub-catchments that lose direct glacier–wetland connectivity rely increasingly on rainfall, resulting in more pronounced seasonality and greater sensitivity to dry-season moisture deficits. This rapid spatial transition from meltwater-buffered to precipitation-dominated wetlands reveals that glacier–wetland linkages are limited to a relatively narrow upstream zone. Ongoing glacier retreat will therefore most likely have only very localized impacts on wetlands.

Methodologically, our remote-sensing and regression framework provides a scalable approach to resolve spatial heterogeneity in wetland–glacier and wetland–climate linkages, even though it cannot directly distinguish individual water sources or subsurface pathways. By revealing systematic distance-dependent gradients in glacier influence, our study shows how such a spatially explicit landscape–system approach can help to assess highly localized wetland–glacier connectivity.

Conflict of Interest

The authors declare no conflicts of interest relevant to this study.

Availability Statement

The data, code, and results used in the study are available at Zenodo via https://doi.org/10.5281/zenodo.18261913 with Creative Commons Attribution 4.0 International (Xuan et al., 2026).

Acknowledgments
We thank the two anonymous reviewers for their constructive comments and suggestions, which helped improve the clarity and quality of this manuscript. This work was supported by the Natural Environment Research Council highlight topic grant Deplete and Retreat (NE/X004031/1), to J. C. Ely, W. Buytaert and B. Davies, and which supported R. Becker and O. King.

References

Baraer, M., Mark, B. G., McKenzie, J. M., Condom, T., Bury, J., Huh, K.-I., et al. (2012). Glacier recession and water resources in Peru's Cordillera Blanca. *Journal of Glaciology*, *58*(207), 134–150. https://doi.org/10.3189/2012jog11j186

Becker, R., Kropáček, J., Ross, A. C., Gribbin, T., Drenkhan, F., Sotelo, L. H., & Buytaert, W. (2026). A map of high-altitude wetlands in the world's major mountain regions. *Scientific Data*.

Buytaert, W., Célleri, R., De Bièvre, B., Cisneros, F., Wyseure, G., Deckers, J., & Hofstede, R. (2006). Human impact on the hydrology of the Andean Páramos. *Earth-Science Reviews*, *79*(1–2), 53–72. https://doi.org/10.1016/j.earscirev.2006.06.002

Buytaert, W., Moulds, S., Acosta, L., De Bièvre, B., Olmos, C., Villacis, M., et al. (2017). Glacial melt content of water use in the tropical Andes. *Environmental Research Letters*, *12*(11), 114014. https://doi.org/10.1088/1748-9326/aa926c

Chatterjee, A., Blom, E., Gujja, B., Jacimovic, R., Beevers, L., O'Keeffe, J., et al. (2010). WWF initiatives to study the impact of climate change on Himalayan high-altitude wetlands (HAWs). *Mountain Research and Development*, *30*(1), 42–52. https://doi.org/10.1659/mrd-journal-d-09-00091.1

Chesnokova, A., Baraër, M., Laperrière-Robillard, T., & Huh, K. (2020). Linking mountain glacier retreat and hydrological changes in southwestern Yukon. *Water Resources Research*, *56*(1), e2019WR025706. https://doi.org/10.1029/2019wr025706

Chimner, R. A., Lemly, J. M., & Cooper, D. J. (2010). Mountain fen distribution, types and restoration priorities, San Juan Mountains, Colorado, USA. *Wetlands*, *30*(4), 763–771. https://doi.org/10.1007/s13157-010-0039-5

Chimner, R. A., Resh, S. C., Hribljan, J. A., Battaglia, M., Bourgeau-Chavez, L., Bowser, G., & Lilleskov, E. A. (2023). Mountain wetland soil carbon stocks of Huascarán National Park, Peru. *Frontiers in Plant Science*, *14*, 1048609. https://doi.org/10.3389/fpls.2023.1048609

Cooper, D. J., Sueltenfuss, J., Oyague, E., Yager, K., Slayback, D., Caballero, E. M. C., et al. (2019). Drivers of peatland water table dynamics in the central Andes, Bolivia and Peru. *Hydrological Processes*, *33*(13), 1913–1925. https://doi.org/10.1002/hyp.13446

Dangles, O., Rabatel, A., Kraemer, M., Zeballos, G., Soruco, A., Jacobsen, D., & Anthelme, F. (2017). Ecosystem sentinels for climate change? Evidence of wetland cover changes over the last 30 years in the tropical Andes. *PLoS One*, *12*(5), e0175814. https://doi.org/10.1371/journal.pone.0175814

Davies, B., Gribbin, T., King, O., Matthews, T., Baiker, J. R., Becker, R., et al. (2026). Landsystems of the tropical high Peruvian Andes: Glaciers, lakes, wetlands and water resources in the Cordillera Vilcanota. *Earth Surface Processes and Landforms*, *51*(5), e70296. https://doi.org/10.1002/esp.70296

de la Fuente, A., Meruane, C., & Suárez, F. (2021). Long-term spatiotemporal variability in high Andean wetlands in northern Chile. *Science of the Total Environment*, *756*, 143830. https://doi.org/10.1016/j.scitotenv.2020.143830

Dinerstein, E., Olson, D., Joshi, A., Vynne, C., Burgess, N. D., Wikramanayake, E., et al. (2017). An ecoregion-based approach to protecting half the terrestrial realm. *BioScience*, *67*(6), 534–545. https://doi.org/10.1093/biosci/bix014

Drenkhan, F., Carey, M., Huggel, C., Seidel, J., & Oré, M. T. (2015). The changing water cycle: Climatic and socioeconomic drivers of water-related changes in the Andes of Peru. *Wiley Interdisciplinary Reviews: Water*, *2*(6), 715–733. https://doi.org/10.1002/wat2.1105

Emmer, A. (2024). Infilled lakes (P ampas) of the Cordillera Blanca, Peru: Inventory, sediment storage, and paleo outbursts. *Progress in Physical Geography: Earth and Environment*, *48*(2), 208–230. https://doi.org/10.1177/03091333241227799

Fyffe, C. L., Potter, E., Fugger, S., Orr, A., Fatichi, S., Loarte, E., et al. (2021). The energy and mass balance of Peruvian glaciers. *Journal of Geophysical Research: Atmospheres*, *126*(23), e2021JD034911. https://doi.org/10.1029/2021jd034911

Glas, R., Lautz, L., McKenzie, J., Mark, B., Baraer, M., Chavez, D., & Maharaj, L. (2018). A review of the current state of knowledge of proglacial hydrogeology in the Cordillera Blanca, Peru. *Wiley Interdisciplinary Reviews: Water*, *5*(5), e1299. https://doi.org/10.1002/wat2.1299

Gribbin, T., Mackay, J. D., MacDonald, A., Hannah, D. M., Buytaert, W., Baiker, J. R., et al. (2024). Bofedal wetland and glacial melt contributions to dry season streamflow in a high-Andean headwater watershed. *Hydrological Processes*, *38*(8), e15237. https://doi.org/10.1002/hyp.15237

Haeberli, W., & Weingartner, R. (2020). In full transition: Key impacts of vanishing mountain ice on water-security at local to global scales. *Water Security*, *11*, 100074. https://doi.org/10.1016/j.wasec.2020.100074

Huffman, G. J., Bolvin, D. T., Braithwaite, D., Hsu, K., Joyce, R., & Xie, P. (2014). *Integrated multi-satellite retrievals for GPM (IMERG)*. Precipitation Measurement Missions Technical documentation.

Huss, M., & Hock, R. (2018). Global-scale hydrological response to future glacier mass loss. *Nature Climate Change*, *8*(2), 135–140. https://doi.org/10.1038/s41558-017-0049-x

INAIGEM. (2023a). *Memoria Descriptiva del Inventario Nacional de Bofedales del Perú 2023* (Tech. Rep.). Huaraz, Perú: Instituto Nacional de Investigación en Glaciares y Ecosistemas de Montaña.

INAIGEM. (2023b). *Memoria descriptiva del Inventario Nacional de Glaciares y Lagunas de Origen Glaciar del Perú* (Tech. Rep.). Huaraz, Perú: Dirección de Investigación en Glaciares (DIG) - Instituto Nacional de Investigación en Glaciares y Ecosistemas de Montaña (INAIGEM).

Maldonado, M. (2014). An introduction to the bofedales of the Peruvian High Andes. *Mires & Peat*, *15*(5), 1–13.

Maldonado-Fonkén, M., Chuquillanqui, H., Vildoso, B., & Linares-Palomino, R. (2024). Plant communities of high-Andean bofedal wetlands across a trans-Andean transect in southern Peru. In *Vegetation classification and survey* (Vol. 5, pp. 203–218). https://doi.org/10.3897/vcs.115726

Mark, B. G., & Mckenzie, J. M. (2007). Tracing increasing tropical Andean glacier melt with stable isotopes in water. *Environmental Science & Technology*, *41*(20), 6955–6960. https://doi.org/10.1021/es071099d

Marquardt, D. W., & Snee, R. D. (1975). Ridge regression in practice. *The American Statistician*, *29*(1), 3–20. https://doi.org/10.1080/00031305.1975.10479105

Marzeion, B., Hock, R., Anderson, B., Bliss, A., Champollion, N., Fujita, K., et al. (2020). Partitioning the uncertainty of ensemble projections of global glacier mass change. *Earth's Future*, *8*(7), e2019EF001470. https://doi.org/10.1029/2019ef001470

McDonald, G. C. (2009). Ridge regression. *Wiley Interdisciplinary Reviews: Computational Statistics*, *1*(1), 93–100. https://doi.org/10.1002/wics.14

Monge-Salazar, M. J., Tovar, C., Cuadros-Adriazola, J., Baiker, J. R., Montesinos-Tubüe, D. B., Bonnesoeur, V., et al. (2022). Ecohydrology and ecosystem services of a natural and an artificial bofedal wetland in the central Andes. *Science of the Total Environment*, *838*, 155968. https://doi.org/10.1016/j.scitotenv.2022.155968

Mountain Research Initiative EDW Working Group. (2015). Elevation-dependent warming in mountain regions of the world. *Nature Climate Change*, *5*(5), 424–430. https://doi.org/10.1038/nclimate2563

Muñoz-Sabater, J., Dutra, E., Agustí-Panareda, A., Albergel, C., Arduini, G., Balsamo, G., et al. (2021). ERA5-Land: A state-of-the-art global reanalysis dataset for land applications. *Earth System Science Data*, *13*(9), 4349–4383. https://doi.org/10.5194/essd-13-4349-2021

Ó Dochartaigh, B. É., MacDonald, A. M., Black, A. R., Everest, J., Wilson, P., Darling, W. G., et al. (2019). Groundwater–glacier meltwater interaction in proglacial aquifers. *Hydrology and Earth System Sciences*, *23*(11), 4527–4539. https://doi.org/10.5194/hess-23-4527-2019

Oyague, E., & Cooper, D. J. (2020). Peatlands of the central Andes Puna, South America. *Wetland Science & Practice*, *37*(4), 255–260. https://doi.org/10.1672/ucrt083-204

Oyague, E., Cooper, D. J., & Ingol, E. (2022). Effects of land use on the hydrologic regime, vegetation, and hydraulic conductivity of peatlands in the central Peruvian Andes. *Journal of Hydrology*, *609*, 127687. https://doi.org/10.1016/j.jhydrol.2022.127687

Pfeffer, W. T., Arendt, A. A., Bliss, A., Bolch, T., Cogley, J. G., Gardner, A. S., et al. (2014). The Randolph Glacier Inventory: A globally complete inventory of glaciers. *Journal of Glaciology*, *60*(221), 537–552. https://doi.org/10.3189/2014jog13j176

Polk, M. H., Young, K. R., Baraer, M., Mark, B. G., McKenzie, J. M., Bury, J., & Carey, M. (2017). Exploring hydrologic connections between tropical mountain wetlands and glacier recession in Peru's Cordillera Blanca. *Applied Geography*, *78*, 94–103. https://doi.org/10.1016/j.apgeog.2016.11.004

Radić, V., Bliss, A., Beedlow, A. C., Hock, R., Miles, E., & Cogley, J. G. (2014). Regional and global projections of twenty-first century glacier mass changes in response to climate scenarios from global climate models. *Climate Dynamics*, *42*(1), 37–58. https://doi.org/10.1007/s00382-013-1719-7

RGI Consortium. (2023). *Randolph Glacier Inventory (RGI)—A dataset of global glacier outlines, version 7.0*. NSIDC: National Snow and Ice Data Center. https://doi.org/10.5067/F6JMOVY5NAVZ

Rojas, Y., & Minder, J. R. (2024). Variability of the Southern Andes rain shadow. *Atmospheric Research*, *308*, 107509. https://doi.org/10.1016/j.atmosres.2024.107509

Ross, A. C., Mendoza, M. M., Drenkhan, F., Montoya, N., Baiker, J. R., Mackay, J. D., et al. (2023). Seasonal water storage and release dynamics of bofedal wetlands in the Central Andes. *Hydrological Processes*, *37*(8), e14940. https://doi.org/10.1002/hyp.14940

Strahler, A. N. (1957). Quantitative analysis of watershed geomorphology. *EOS Transactions of the American Geophysical Union*, *38*(6), 913–920.

Taylor, L. S., Quincey, D. J., Smith, M. W., Potter, E. R., Castro, J., & Fyffe, C. L. (2022). Multi-decadal glacier area and mass balance change in the southern Peruvian Andes. *Frontiers in Earth Science*, *10*, 863933. https://doi.org/10.3389/feart.2022.863933

Verzijl, A., & Quispe, S. G. (2013). The system nobody sees: Irrigated wetland management and alpaca herding in the Peruvian Andes. *Mountain Research and Development*, *33*(3), 280–293. https://doi.org/10.1659/mrd-journal-d-12-00123.1

Wunderlich, W., Lang, M., Keating, K., Perez, W. B., & Oshun, J. (2023). The role of peat-forming bofedales in sustaining baseflow in the humid puna. *Journal of Hydrology: Regional Studies*, *47*, 101394. https://doi.org/10.1016/j.ejrh.2023.101394

Xuan, D., Becker, R., & Buytaert, W. (2026). Spatial patterns of glacier meltwater and mountain wetland connectivity in the Peruvian Andes [Dataset]. *Zenodo*. https://doi.org/10.5281/zenodo.18261913

Zekollari, H., Schuster, L., Maussion, F., Hock, R., Marzeion, B., Rounce, D. R., et al. (2025). Glacier preservation doubled by limiting warming to 1.5°C versus 2.7°C. *Science*, *388*(6750), 979–983. https://doi.org/10.1126/science.adu4675

Zemp, M., Frey, H., Gärtner-Roer, I., Nussbaumer, S. U., Hoelzle, M., Paul, F., et al. (2015). Historically unprecedented global glacier decline in the early 21st century. *Journal of Glaciology*, *61*(228), 745–762. https://doi.org/10.3189/2015jog15j017

References From the Supporting Information

Becker, R., & Buytaert, W. (2025). A map of high mountain wetlands in the world's major mountain regions [Dataset]. *Zenodo*. https://doi.org/10.5281/zenodo.14930773

Funk, C., Peterson, P., Landsfeld, M., Pedreros, D., Verdin, J., Shukla, S., et al. (2015). The climate hazards infrared precipitation with stations—A new environmental record for monitoring extremes. *Scientific Data*, *2*(1), 150066. https://doi.org/10.1038/sdata.2015.66

Gogtay, N. J., & Thatte, U. M. (2017). Principles of correlation analysis. *Journal of the Association of Physicians of India*, *65*(3), 78–81.

Grömping, U. (2007). Estimators of relative importance in linear regression based on variance decomposition. *The American Statistician*, *61*(2), 139–147. https://doi.org/10.1198/000313007x188252

Hastie, T., Tibshirani, R., & Friedman, J. (2009). *The elements of statistical learning*. Springer Series in Statistics. https://doi.org/10.1007/978-0-387-84858-7

Huffman, G. J., Bolvin, D. T., Nelkin, E. J., & Tan, J. (2015). Integrated Multi-satellitE Retrievals for GPM (IMERG) technical documentation. *NASA/GSFC Code*, *612*(47), 2019.

Huffman, G. J., Bolvin, D. T., Braithwaite, D., Hsu, K.-L., Joyce, R. J., Kidd, C., et al. (2020). Integrated multi-satellite retrievals for the global precipitation measurement (GPM) mission (IMERG). In *Satellite precipitation measurement* (Vol. 1, pp. 343–353). Springer.

Karger, D. N., Conrad, O., Böhner, J., Kawohl, T., Kreft, H., Soria-Auza, R. W., et al. (2017). Climatologies at high resolution for the earth's land surface areas. *Scientific Data*, *4*(1), 1–20. https://doi.org/10.1038/sdata.2017.122

López-Vicente, M., Pérez-Bielsa, C., López-Montero, T., Lambán, L. J., & Navas, A. (2014). Runoff simulation with eight different flow accumulation algorithms: Recommendations using a spatially distributed and open-source model. *Environmental Modelling & Software*, *62*, 11–21. https://doi.org/10.1016/j.envsoft.2014.08.025

Zhang, W., Li, W., Loaiciga, H. A., Liu, X., Liu, S., Zheng, S., & Zhang, H. (2021). Adaptive determination of the flow accumulation threshold for extracting drainage networks from DEMs. *Remote Sensing*, *13*(11), 2024. https://doi.org/10.3390/rs13112024